Biosensors and Bioelectronics 80 (2016) 24–33

Contents lists available at ScienceDirect

Biosensors and Bioelectronics

journal homepage: www.elsevier.com/locate/bios

Electrochemical magnetic microbeads-based biosensor for point-of-care serodiagnosis of infectious diseases

María E. Cortina [a,1], Luciano J. Melli [a,1], Mariano Roberti [c], Mijal Mass [c], Gloria Longinotti [b], Salvador Tropea [c], Paulina Lloret [b], Diego A. Rey Serantes [a], Francisco Salomón [c], Matías Lloret [c], Ana J. Caillava [a], Sabrina Restuccia [b], Jaime Altcheh [d], Carlos A. Buscaglia [a], Laura Malatto [c], Juan E. Ugalde [a], Liliana Fraigi [c], Carlos Moina [b], Gabriel Ybarra [b,*], Andrés E. Ciocchini [a,**], Diego J. Comerci [a,e,***]

[a] Instituto de Investigaciones Biotecnológicas "Dr. Rodolfo A. Ugalde", Instituto Tecnológico de Chascomús (IIB-INTECH), Universidad Nacional de San Martín, CONICET, San Martín, Buenos Aires, Argentina
[b] U.T. Nanomateriales, Centro INTI-Procesos Superficiales, Instituto Nacional de Tecnología Industrial, Buenos Aires, Argentina
[c] Centro de Micro y Nanoelectrónica del Bicentenario, Instituto Nacional de Tecnología Industrial, Buenos Aires, Argentina
[d] Parasitología-Chagas, Hospital de Niños Ricardo Gutiérrez, Buenos Aires, Argentina
[e] Comisión Nacional de Energía Atómica, Grupo Pecuario, Centro Atómico Ezeiza, Buenos Aires, Argentina

ARTICLE INFO

Article history:
Received 23 November 2015
Received in revised form
23 December 2015
Accepted 7 January 2016
Available online 14 January 2016

Keywords:
Point-of-Care diagnosis
Electrochemical biosensor
Magnetic-beads
Recombinant antigens
Infectious diseases

ABSTRACT

Access to appropriate diagnostic tools is an essential component in the evaluation and improvement of global health. Additionally, timely detection of infectious agents is critical in early diagnosis and treatment of infectious diseases. Conventional pathogen detection methods such as culturing, enzyme linked immunosorbent assay (ELISA) or polymerase chain reaction (PCR) require long assay times, and complex and expensive instruments making them not adaptable to point-of-care (PoC) needs at resource-constrained places and primary care settings. Therefore, there is an unmet need to develop portable, simple, rapid, and accurate methods for PoC detection of infections. Here, we present the development and validation of a portable, robust and inexpensive electrochemical magnetic microbeads-based biosensor (EMBIA) platform for PoC serodiagnosis of infectious diseases caused by different types of microorganisms (parasitic protozoa, bacteria and viruses). We demonstrate the potential use of the EMBIA platform for *in situ* diagnosis of human (Chagas disease and human brucellosis) and animal (bovine brucellosis and foot-and-mouth disease) infections clearly differentiating infected from non-infected individuals or animals. For Chagas disease, a more extensive validation of the test was performed showing that the EMBIA platform displayed an excellent diagnostic performance almost indistinguishable, in terms of specificity and sensitivity, from a fluorescent immunomagnetic assay and the conventional ELISA using the same combination of antigens. This platform technology could potentially be applicable to diagnose other infectious and non-infectious diseases as well as detection and/or quantification of biomarkers at the POC and primary care settings.

1. Introduction

Access to appropriate diagnostic tools is an essential component in the evaluation and improvement of global health (Girosi et al., 2006; Hay Burgess et al., 2006). Diagnostics are crucial for identifying the presence and cause of disease at the individual and population levels, both in humans and animals. In addition, timely detection of infectious agents is critical in early diagnosis and treatment of infectious diseases. Conventional pathogen detection methods such as culturing, enzyme linked immunosorbent assay (ELISA) or polymerase chain reaction (PCR) require relatively

* Corresponding author.
** Corresponding author.
*** Corresponding author at: Instituto de Investigaciones Biotecnológicas "Dr. Rodolfo A. Ugalde", Instituto Tecnológico de Chascomús (IIB-INTECH), Universidad Nacional de San Martín, CONICET, Campus Miguelete, Av. 25 de Mayo y Francia, San Martín CP 1650, Provincia de Buenos Aires, Argentina.
E-mail addresses: gabriel@inti.gob.ar (G. Ybarra), aciocchini@iibintech.com.ar (A.E. Ciocchini), dcomerci@iibintech.com.ar (D.J. Comerci).
[1] These authors contributed equally to this work.

http://dx.doi.org/10.1016/j.bios.2016.01.021
0956-5663/

sophisticated infrastructure and well-equipped laboratories, and must be performed by highly trained staff, conditions that make them not adaptable to point-of-care (PoC) needs at resource-constrained and primary care settings (Song et al., 2014; Urdea et al., 2006). Additionally, many current diagnostic tools require more than one visit of the patients to the health care units, which is complicated or not possible for many people in developing countries, especially for those living far away from the health centers. Therefore, there is an increasing interest in developing portable, simple, rapid, and accurate methods for detection of pathogens at the PoC. The implementation of rapid, specific and reliable PoC devices for the in situ diagnosis, mass-screening surveys and/or intervention campaigns (e.g., during the onset of outbreaks) in endemic areas could significantly improve the diagnostic and clinical management fields, particularly for tropical and/or neglected diseases (Peeling and Mabey, 2010).

The biosensors are the ideal systems to address all those requirements and frequently offer a good response in terms of reliability, analytical performance and mass-screening. Furthermore, biosensors with high degree of integration are more amenable for mass production offering a better and more reproducible response. In the last years, optical, electrochemical and piezoelectric biosensors devices have emerged as important tools capable of improving detection of a variety of analytes (Bănică, 2012; Holford et al., 2012). In particular, electrochemical biosensors can be developed with a higher degree of integration than optical biosensors, which require the use of light sources and detectors. Electrochemical transducers have been widely used in biosensors due to their high sensitivity, low cost, simple design and small size making them excellent candidates for the development of portable biosensors (Dorothee Grieshaber et al., 2008).

Most of the biosensing techniques are carried out either on solid-phase supports or biological membranes. Magnetic microspheres have been widely used as a solid-phase support for the detection of biomolecules such as nucleic acids, polypeptides and/or antibodies (Kuramitz, 2009). When coated with antigens, magnetic beads provide an ideal support for serodiagnosis allowing the removal of unwanted sample constituents by a simple magnetic separation step with minimal loss of the target material (Ciocchini et al., 2013; Ciocchini et al., 2014; Iwashkiw et al., 2012). Additionally, magnetic microspheres confer a number of other benefits compared to other solid supports, including relatively large surface-to-volume ratio, high throughput capacity and reproducibility, reduced assay time and small sample volume requirements.

In this work, we have developed and evaluated an electrochemical magnetic microbeads-based biosensor (EMBIA) for PoC serodiagnosis of infection diseases caused by different types of microorganisms (parasitic protozoa, bacteria and viruses) using previously validated recombinant antigens. The EMBIA biosensor or platform includes three main components: antigen-functionalized magnetic microbeads, disposable electrochemical cells-electrode cartridges and a portable potentiostat. In this platform, superparamagnetic microbeads functionalized with the corresponding antigens are sequentially incubated with the samples and the HRP-conjugated antibodies, and the electrochemical readings performed on the 8-channel-electrochemical cells-electrode cartridges using the portable potentiostat. Our data support the potential use of the EMBIA platform for the *in situ* diagnosis of human and animal infectious diseases with an excellent signal-to-noise ratio. In the particular case of Chagas disease, a more extensive validation was performed showing that the EMBIA platform displayed an excellent diagnostic performance, in terms of specificity and sensitivity, almost indistinguishable from a fluorescent immunomagnetic assay and the conventional ELISA using the same combination of recombinant antigens.

2. Material and methods

2.1. Serum samples

2.1.1. Human serum samples

The institutional review board of the corresponding institutions approved the use of serum samples in the current study. Written informed consent was obtained from all individuals. Serum samples were collected from clotted blood obtained by venipuncture and stored at −20 °C, and were decoded and de-identified before they were provided for research purposes. Therefore, no information (e.g., name, age, sex, etc.) regarding the patients was available.

A total of 78 positive samples obtained from Chagas disease patients coursing the chronic phase of the disease (positive reference samples) were analyzed. Of the 78 positive samples 46 were obtained from our own collection and were described elsewhere (Balouz et al., 2015; Di Noia et al., 2002). These samples were positive by three independent assays: ELISA using total parasite homogenate, Indirect Hemagglutination Assay (IHA) and Indirect Immunofluorescence (IIF). The remaining 32 samples were provided by the Laboratorio de Enfermedad de Chagas, Hospital de Niños “Dr. Ricardo Gutierrez” (Buenos Aires, Argentina). These samples were positive by ELISA using total parasite homogenate (Wiener lab, Argentina) and IHA (Polychaco, Argentina).

For diagnosis of human brucellosis, 17 serum samples, from a previously characterized sera collection provided by the Brucellosis Division from the Hospital de Enfermedades Infecciosas Francisco Javier Muñiz (Buenos Aires, Argentina), were analyzed (Ciocchini et al., 2013). These samples were obtained from patients with positive blood culture for *Brucella abortus*, *Brucella melitensis* or *Brucella suis* and serologically-positive by the following serological tests currently used for diagnosis of the disease: Rose Bengal Test (RBT), Serum Agglutination Test (SAT; Huddleson), Tube Agglutination Test (TAT; Wright), TAT-2ME (2-mercaptoethanol), Competitive ELISA (CELISA) and Complement Fixation Test (CFT).

A total of 122 negative samples were obtained from healthy blood donors. These samples, considered as negative reference samples for Chagas disease and human brucellosis, were negative in routine screening tests for both diseases. Of the 122 negative samples, 59 were obtained from the "Fundación Hemocentro Buenos Aires" (Buenos Aires, Argentina), 27 from the Hospital de Enfermedades Infecciosas “Dr. Francisco Javier Muñiz” (Buenos Aires, Argentina), 16 from Hospital Italiano de Buenos Aires (Buenos Aires, Argentina) and 20 from the Hospital Municipal “Dr. Diego E. Thompson” (San Martín, Buenos Aires, Argentina).

2.1.2. Bovine serum samples

All animal serum samples were provided by the National Brucellosis Reference Laboratory (DILAB-SENASA) from Argentina. Twelve serum samples obtained from naturally *B. abortus*-infected bovines were analyzed (Ciocchini et al., 2014). These samples were serologically positive by the serological tests currently used for diagnosis of the disease: Buffer Plate Agglutination Test (BPAT), SAT, CELISA, indirect ELISA (iELISA), Fluorescent Polarization Assay (FPA) and CFT. Fifteen positive serum samples obtained from cows with clinical signs of foot-and-mouth disease (FMD) and serologically positive by 3ABC-iELISA and confirmed by Electro-ImmunoTransfer Blotting technique (EITB) were analyzed. Twenty-three serum samples obtained from officially certified brucellosis and FMD-free herds were used as negative reference samples. These samples resulted negative in routine screening tests for both diseases (BPAT for bovine brucellosis, and 3ABC-iELISA for FMD).

2.2. Production and purification of recombinant antigens

Plasmids and bacterial strains used in this work are listed in Table S1.

2.2.1. T. cruzi antigens (GST-Ag1, GST-Ag36, GST-SAPA and GST-TSSA)

A panel of validated *T. cruzi* antigens, for which the performance in Chagas disease serodiagnosis has been already reported, was used (see supplemental material). Ag1, Ag36 and SAPA constructs were subcloned in pGEX1λT expression vector (GE Healthcare Life Sciences), which provides translational fusion to Glutathione *S*-transferase (GST) protein, from the plasmids pTrcHis-TS-Ag1, pTrcHis-TS-Ag36 and pTrcHis-TS-SAPA, respectively (Buscaglia et al., 1999). Briefly, these constructs were excised from pTrcHis vector (Invitrogen) by *Eco*RI digestion and subsequently ligated into pGEX1λT. Cloning of the predicted mature product (i.e., without most of the endoplasmic reticulum and GPI anchor signals) of the *TSSA* gene from the CL Brener clone (GenBank accession number ACY54510) into the plasmid pGEX2T has been previously described (De Marchi et al. 2011). *Escherichia coli* DH5αF'IQ™ (Life Technologies) strain was used for all the cloning procedures. All constructs were further analyzed by DNA sequencing (Applied Biosystems ABI3130 capillary sequencer). For expression and purification of the antigens, the *E. coli* BL21-CodonPlus (DE3)-RP strain was transformed with the plasmids pGEX1λT-Ag1, pGEX1λT-Ag36, pGEX1λT-SAPA or pGEX2T-TSSA. The resulting strains were grown overnight at 37 °C with agitation in Luria-Bertani (LB) broth supplemented with 20 g/mL chloramphenicol and 100 g/mL ampicillin, and re-inoculated at 1:100 dilution into fresh LB medium. After incubation for 3 h at 37 °C ($OD_{600} \approx 0.5$), protein expression was induced by addition of isopropyl-α-D thiogalactopyranoside (IPTG) to a final concentration of 1 mM. Following a 3 h-induction period, cells were harvested by centrifugation and cytoplasmic extracts were obtained by lysing the cells with lysis buffer (50 mM Tris–HCl pH 7.6, 150 mM NaCl, 0.5% Triton X-100, 0.5 mg/mL lysozyme, 10 mM $MgCl_2$, 2 mM PMSF, 2 mM EDTA and 10 μg/mL DNase) and sonication. After centrifugation, the soluble fraction was subjected to glutathione-Sepharose affinity chromatography following the manufacturer's instructions (GE Healthcare Life Sciences).

2.2.2. Brucella antigen (OAg-AcrA)

Production and purification of the OAg-AcrA glycoconjugate was performed as previously described (Ciocchini et al., 2013, 2014; Iwashkiw et al., 2012). Briefly, *Yersinia enterocolitica* O:9 wild type strain transformed with the plasmids pMAF10 (encoding the *Campylobacter jejuni* oligosaccharyltransferase PglB) and pMH5 (encoding the *C. jejuni* carrier protein AcrA fused to a 6x histidine tag) was grown overnight at 37 °C. Cultures were re-inoculated at 1:100 dilution into fresh LB medium and grown at 37 °C for 2.5 h ($OD_{600} \approx 0.5$) and PglB expression was induced by addition of arabinose to a final concentration of 0.2% (w/v). Four hours after induction at 37 °C, PglB was re-induced by a second addition of arabinose to maximize glycosylation of AcrA. Cells were harvested by centrifugation after a 20 h induction period and periplasmic extracts were prepared by lysozyme treatment and the glycoprotein purified by Immobilized Metal Affinity Chromatography (IMAC) following the manufacturer's instructions (GE Healthcare Life Sciences).

2.2.3. FMDV antigen (3ABC)

Total RNA of the strain FMDV 01 Campos was extracted using the Trizol® reagent (Life Technologies) according to the manufacturer instructions. cDNA synthesis was performed using the ThermoScript RT-PCR System (Life Technologies) and the 3ABC gene was amplified by PCR using Pfx DNA polymerase (Life Technologies) and the oligonucleotides *Nde*I-3ABC (CGCATATGATCTCAATTCCTTCCCAA, underlined sequence indicates the restriction site) and 3ABC-*Hind*III (CCAAGCTTCTCGTGGTGTGGTGGTTCGGG). The amplified DNA fragment was digested with *Nde*I and *Hind*III and cloned into the plasmid pET22b (+) (Novagen) previously digested with the same enzymes. The resulting plasmid was named pET22b-3ABC. Subsequently *E. coli* BL21-CodonPlus (DE3)-RP strain was transformed with the plasmid pET22b-3ABC and the resulting strain was grown overnight at 37 °C with agitation in LB medium supplemented with 20 g/mL chloramphenicol and 100 g/mL ampicillin, and re-inoculated at 1:100 dilution into fresh LB medium. After incubation for 3 h at 37 °C ($OD_{600} \approx 0.5$), protein expression was induced by addition of IPTG to a final concentration of 1 mM. After induction for 18 h at 18 °C, cells were harvested by centrifugation and the cytoplasmic extracts were obtained by incubating the cells with lysis buffer (see above) and sonication. After centrifugation, the soluble fraction was subjected to Immobilized Metal Affinity Chromatography (IMAC) following the manufacturer's instructions (GE Healthcare Life Sciences).

All the purified antigens were dialyzed against 0.01 M phosphate-buffered saline pH 7.2 (PBS), quantified by Bradford's protein assay and analyzed by Coomassie brilliant blue-stained SDS-PAGE and Western blotting (data not shown).

2.3. Coating of superparamagnetic microbeads

Superparamagnetic COOH-modified microbeads (5% solids, 7.9 μm, Bangs Laboratories) were activated in one step with NHS [N-hydroxysuccinimide] in 100 mM MES [2-(N-Morpholino) ethanesulfonic acid] pH 5.5 buffer and EDAC [1-ethyl-3-(3-dimethyl-aminopropyl) carbodiimide hydrochloride]. Activated beads were washed with PBS and incubated for three hours with different amounts of GST-Ag1, GST-Ag36, GST-SAPA, GST-TSSA, OAg-AcrA or 3ABC. One mL of antigen solution (0.05 to 0.2 mg/mL) was incubated with 0.25 mL of beads suspension, thus yielding enough material for 50 reactions (see below). Coated magnetic beads were washed with quenching buffer (35 mM glycine, 1% gelatin from cold-water fish skin) and incubated overnight at 4 °C with the same buffer and orbital agitation. Finally, coated beads were washed with storage buffer (1% gelatin from cold-water fish skin, 2.25% Tween 20, 0.01% sodium azide), resuspended in 1 mL of the same buffer and stored at 4 °C until use.

2.4. Electrochemical enzyme-linked magnetic beads immunoassay (EMBIA): principle of the assay and optimization

Antigen-coated magnetic beads were incubated with human or bovine serum samples, washed three times with PBS containing 0.2% Tween 20 (PBST) and bound antibodies were detected with horseradish peroxidase (HRP)-conjugated goat anti-human IgG (Sigma-Aldrich) or HRP-conjugated goat anti-bovine IgG (H+L, Jackson ImmunoResearch Laboratories) antibodies. After washing three times with PBST, the beads were resuspended in PBS and transferred to the electrochemical cells (disposable cartridges with eight electrodes and electrochemical cells, see below). In the cartridge, the particles a magnetically collected and placed onto the surface of the electrode. After adding the substrate (1.5 mM H_2O_2) and 4 mM hydroquinone in PBS, peroxidase activity was amperometrically recorded using a mini-portable potentiostat. The electrode potential was set at −0.23 V and the resulting current recorded for 20 s. The instant limit current at 20 s was used as a measure of the reactivity. Potentials were measured and referred against an Ag|AgCl|0.1 M KCl reference electrode. Washes between incubation steps were performed using a magnetic rack without the need of centrifugation (Fig. 1). Optimization of the assay was performed by a checkerboard titration analysis. Based on these

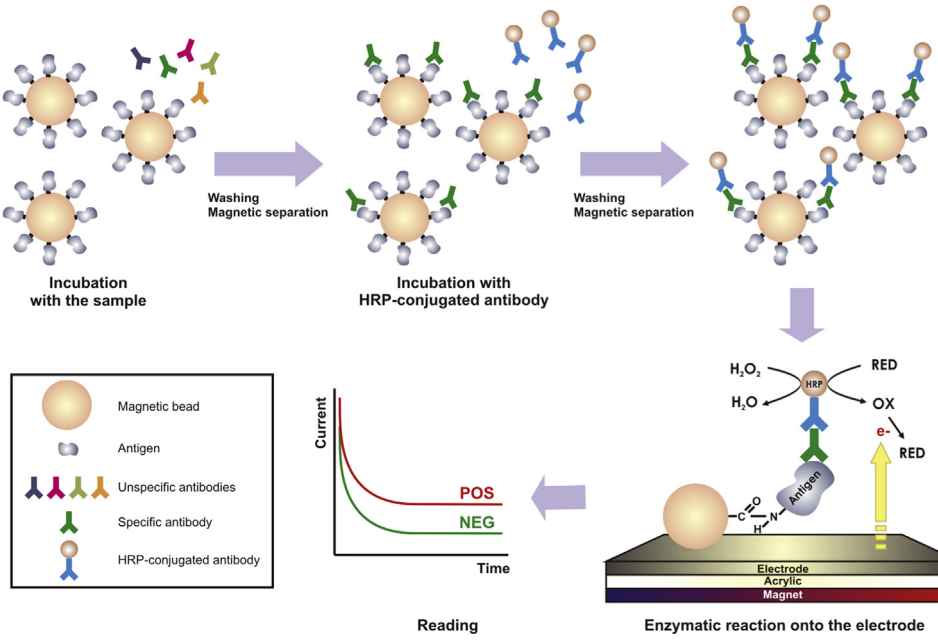

Fig. 1. Schematic representation of the electrochemical enzyme-linked magnetic beads immunoassay and detection principle. Antigen-coated magnetic particles are incubated with the serum samples, washed and then incubated with HRP-conjugated secondary antibodies. After washing, the particles are magnetically collected and placed onto the surface of the electrode. Peroxidase activity is amperometrically recorded using an 8-channel portable potentiostat after adding H_2O_2 and hydroquinone as the substrate and redox mediator, respectively. All incubation and washing steps are performed in 8-tube strips using a magnetic rack without the need of centrifugation.

analyses, the optimal conditions for the EMBIA were: (a) 2 μg of antigen per reaction (in the case of *T. cruzi antigens* 0.5 μg each of the four antigens); (b) 20 μL of coated beads per reaction (in the case of *T. cruzi* antigens, 5 μl of microbeads functionalized with each antigen were mixed); (c) 1:100 dilution of the serum samples; (d) 1:5,000 dilution of the secondary antibodies and (e) 5 min of incubation (at room temperature without agitation) of coated beads with serum samples and conjugate antibodies. These conditions were used to test all the samples.

2.5. Hardware design and development

An 8-channel portable potentiostat was developed to carry out measurements of potentiostatic steps and cyclic voltammetry (Fig. 2A). The device can be controlled via Bluetooth using a set of basic commands. The instrument can control the working electrode voltage in the −2.5 V to +2.5 V range. The valid working electrode current is in the −10 μA and 10 μA range, and the design can be easily adapted for different current ranges. The device is powered by a rechargeable battery and the housing was printed in ABS and designed for electronic protection and error-free cartridges insertion.

2.5.1. Power

A single-cell Li-ion battery (3.7 V) with a charge of 2600 mAh was used which provides more than 9 hours of autonomy continuous measurements. Battery charging control and voltage stepping up to 5 V was implemented using the integrated standalone switching charger ACT2801 which includes an internal boost, protection circuits for high and low voltage, protection

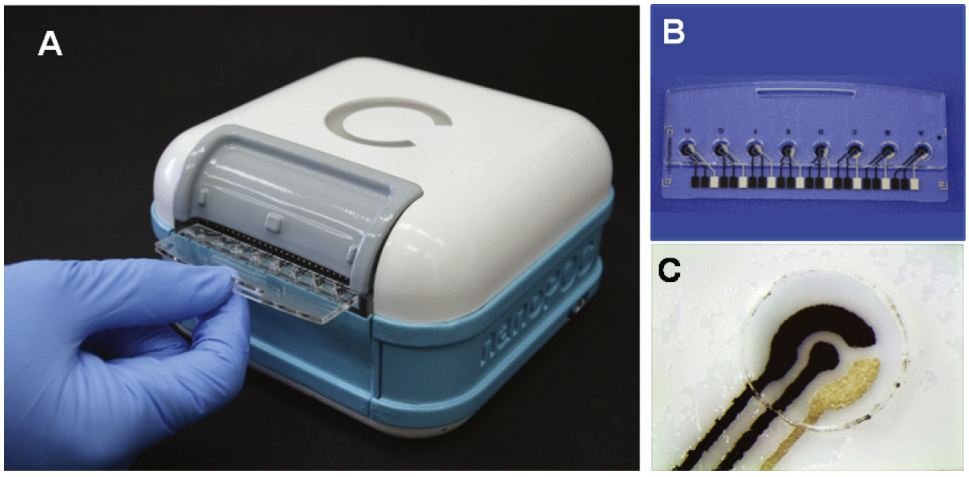

Fig. 2. Portable electrochemical magnetic beads-based platform (EMBIA platform) for PoC diagnosis. (A) Portable 8-channel potentiostat device (nanoPoC). The device, developed to carry out measurements of potentiostatic steps and cyclic voltammetry, can be controlled via Bluetooth using a set of basic commands and is powered by a rechargeable battery. A special designed housing allows error-free cartridge insertion. (B) Acrylic disposable electrochemical cells-electrode cartridge. The disposable acrylic cartridges with eight electrochemical cells were designed and manufactured with dimensions fitting an 8-channel micropipette. (C) Electrodes. Each cell contained two carbon electrodes (working electrode and counter electrode), and one Ag|AgCl reference electrode. The central working electrodes were designed to be aligned with neodymium magnets to allow the concentration of the magnetic particles on the surface of the electrode.

against over temperature and short circuit. Due to the bipolar voltage range required, a dual output DC/DC converter module NMA0509SC was used to power analog circuitry. This module provides −9 V and +9 V outputs from 5 V provided by the ACT2801.

2.5.2. Analog circuitry

Electrodes control and signal conditioning for a single electrochemical cell were carried out using two different types of precision operational amplifier (OPAM). A low offset OPAM OP07 was used to control the counter electrode. To avoid loading reference electrode, an LT1056 JFET input OPAM in buffer configuration was selected, providing an input impedance of (10^{12} Ohms). The current to voltage conversion, carried out in the working electrode circuitry, was also implemented using an LT1056 OPAM in transimpedance amplifier (TIA) configuration. This OPAM introduces a very low current error, typically in the range of 10 pA and guaranteed to be under 0.34 nA for the full operation range. External offset correction was not necessary in any of the cases.

2.5.3. Multiplexing

The eight channels were multiplexed by using two CMOS analog multiplexers DG408 for counter electrode voltage and working electrode current. Reference electrode voltage was not multiplexed due to its floating condition in unused channels and its very high input impedance. Also a circuit with two cheaper analog multiplexer CD4051 was successfully tested.

2.5.4. Control and analog to digital conversion

The potentiostat was controlled by a microcontroller connected to a PC or mobile device via Bluetooth using a HC-06 module. This wireless module provides a serial port profile over Bluetooth V2.0 and was directly connected to the microcontroller to receive serial commands and send acknowledges and data. Checksum error checking was added by firmware. These commands, described in a complete firmware user manual, allows to turn on analog circuitry, channel selection, to configure potential step or voltammetry parameters and limits, start and interrupt assays and others.

Device acknowledge includes error information, and received and transmitted checksum. Microcontroller has a 10 bits A/D converter used to measure the working electrode current and the reference voltage. Counter electrode voltage was controlled with a 12 bits PWM output.

2.6. Electrodes and electrochemical cells

Thick film electrodes were printed onto 0.5 mm acrylic substrates by screen-printing technology. Disposable acrylic cartridges with eight electrochemical cells were designed and manufactured with dimensions fitting an 8-channel micropipette (Fig. 2B). Each cell contained two carbon electrodes (working electrode and counter electrode), and one Ag|AgCl reference electrode (Fig. 2C). Commercial carbon ink (Dupont BQ242), Ag ink (Dupont 5025) and Ag/AgCl ink (Dupont 5870) were used. Electrode layout was transferred by means of photolithography to a stainless steel mesh 200 (wires per inch) with a negative photosensitive film (Ulano CDF-4). All inks printing were performed using an EKRA Microtronic-II printer and dried in a box oven at 70 °C during 20 min. The central working electrodes were designed to be aligned with neodymium magnets to concentrate the magnetic particles. To build the eight electrochemical cells on the same piece where the electrodes were printed, each one with a volume of 40 μl, an acrylic top piece was added.

2.7. Software development

The electronic instrumentation of 8-channel portable potentiostat was developed to communicate with a host device using a serial communication protocol (Fig. S1). The host device can be a PC (e.g., a notebook) or an Android device (e.g., a smartphone or tablet). In order to simplify the validation of this protocol, we implemented a plain text set of commands. In this way, the device could be controlled using a simple terminal emulator software. Wireless Bluetooth communication was chosen to avoid the need of a physical connection with the host and to make possible the use of small host devices such as smartphones. Since Android is the most popular operating system used in small devices (about 80% of market share), an Android application was developed with an easy-to-use user interface.

2.7.1. Test software

A test software for GNU/Linux distributions was developed. It allowed carrying out amperometric records for potential steps and cyclic voltammetry. In both cases, filtering and an optional and configurable preconditioning step was added. The user can select measurement parameters and visualize its evolution in real time. The software can display simultaneously up to eight recorded assays. Back end was developed in C++ language. A full set of classes was written for an object-oriented device management. It manages the equipment connection, sends low level commands, process acknowledges and data, reads calibration constants and others. Perl scripting language and Gtk2 were used for front-end development and communicates with the back end through pipes. This software was useful for general testing, electrodes characterization and particles validation.

2.7.2. Android App

An Android application was also developed in Java language, with complete classes and associated documentation, compatible with API 10 (Android 2.3.3) or greater. Eclipse IDE (Integrated Development Environment) using the ADT (Android Development Tools) plug-in was used to develop the Android application. The app allowed to carry out potential step measurements, setting assay options and threshold presets for different diseases. Furthermore, an Android library was written to provide specific methods related to the device including a specific class for device management that implements the singleton design pattern, ensuring only one instance of the class across the application. The class also allows to register handler objects to receive and process its status connection messages and others. This implementation simplified the software maintenance and future updates, and permits making different applications that manage this device.

When the user starts the application, it searches and connects to a nearby device through an RFCOMM socket by using a secure connection. Once connected, the user triggers an assay and the app sends commands to the device to start a potential step measurement, applying configured voltage in the electrochemical cell and reading work current. The progress of the measurement is displayed on the screen. When the measurement is finished, the app calculates the average value of the work current and indicates the result of the measurement. Additionally, it saves a record for the entire measurement. For the average calculation, only a certain percentage of last samples is considered. A menu button, located at the top right corner, allows the selection of the measurement channels and threshold values.

2.8. Other assays

2.8.1. Fluorescent immunomagnetic assay for Chagas disease

Functionalized microbeads were incubated with human serum

samples, washed three times with PBST and bound antibodies were detected with DyLight 650-conjugated goat anti-human IgG antibodies (Jackson ImmunoResearch Laboratories). After washing three times with PBST, fluorescence was directly determined using a plate fluorometer (DTX 880 Multimode Detector, BeckmanCoulter). Washes between incubation steps were performed using a magnetic rack without the need of centrifugation. In order to determine the optimal conditions for the assay (antigen concentration, sample dilution, secondary antibody dilution, and incubation times), a checkerboard titration analysis was carried out using selected positive (displaying high-, intermediate- and low-reactivity to our panel of recombinant antigens) and negative serum samples. Best results were obtained when using: (a) 0.5 μg of each antigen (GST-Ag1, GST-Ag36, GST-SAPA or GST-TSSA) per reaction (total: 2 μg of antigen per reaction); (b) 20 μL of coated beads per reaction (5 μl of microbeads functionalized with each antigen were mixed); (c) 1:100 dilution of the serum samples; (d) 1:1,000 dilution of the secondary antibodies and (e) 5 min of incubation of coated beads with serum samples and conjugate antibodies (at room temperature without agitation).

2.8.2. Enzyme-linked Immunosorbent Assay (ELISA) for Chagas disease

Polystyrene ELISA high binding microplates (Costar, Corning Incorporated) were coated with 200 ng of a mixture of 50 ng of each antigen (GST-Ag1, GST-Ag36, GST-SAPA and GST-TSSA) in 50 μL of 0.05 M sodium carbonate-bicarbonate buffer (pH 9.6) and incubated at 4 °C overnight. After washing four times with PBST, plates were blocked with PBST supplemented with 5% bovine skim milk (blocking buffer) and incubated for 1 h at 37 °C. Serum samples were diluted 1:200 in blocking buffer and incubated for 1 h at room temperature. After four washes, bound antibodies were detected by the addition of HRP-conjugated goat anti-human IgG antibodies (Sigma-Aldrich) at 1:4,000 dilution in blocking buffer and incubating for 1 h at room temperature. Plates were washed four times with PBST and developed by addition of the substrate-chromogen solution (0.36% H_2O_2 and 0.01% 3,3′,5,5′-Tetramethylbenzidine [TMB] in citrate-phosphate buffer pH 5.0). After 5 min, the reaction was stopped with 2N H_2SO_4 and the absorbance at 450 nanometers was determined using a plate reader (FilterMax Technologies).

2.9. Data analysis

Results of the EMBIA were determined as the average of the last 100 measured values of current (I). Percentage of reactivity was calculated as follows: % of reactivity =(I of the test sample -I of PBST/I of the positive control - I of PBST) × 100. Results of the fluorescent immunomagnetic assay were expressed as percentage of reactivity of the mean Fluorescence Units (FU) of the positive control serum included in each assay run. Percentage of reactivity was calculated as follows: % of reactivity=(FU of the test sample/mean FU of the positive control) × 100. ELISA results were expressed as percentage of reactivity of the mean absorbance at 450 nanometers (Abs450) of the positive control serum included in each assay run. Percentage of reactivity was calculated as follows: % of reactivity=(Abs450 of the test sample/mean Abs450 of the positive control) × 100. Dot and receiver-operating characteristic (ROC) analyses (Greiner and Gardner, 2000; Greiner et al., 1995; Swets, 1988), as well as Mann-Whitney tests were performed using the GraphPad Prism software [version 5.01 for Windows, San Diego California USA, (http://www.graphpad.com)]. ROC analysis allows to determine for each assay the area under the ROC curve (AUC), the cut-off value that concurrently optimizes Se and Sp, the cut-off value for which the diagnostic Se is 100% and the cut-off value that gives a 100% Sp. These latter two cut-off values represent the boundaries of an intermediate range (IR) of reactivity values for definition of indeterminate test results (i.e., those that cannot be conclusively considered either negative or positive under the experimental conditions). The Youden´s index (J) was calculated as Se + Sp − 1; the value of J index is maximal at the cut-off value that concurrently optimizes sensitivity and specificity. Pairwise comparisons of AUCs were performed using the MedCalc Statistical Software version 13.0.6 (MedCalc Software bvba, Ostend, Belgium; http://www.medcalc.org; 2014) (Hanley and McNeil, 1983), and P values < 0.05 were considered significant.

3. Results and discussion

3.1. Characterization of the electrochemical system of the EMBIA platform

The EMBIA platform contains three main components including antigen-functionalized magnetic microbeads, disposable electrochemical cells-electrode cartridges and a portable potentiostat. The detection system of the proposed platform for PoC diagnosis of infectious diseases is based on the capability to detect electrochemically the catalytic activity of enzymes immobilized on the surface of magnetic beads, which are in turn brought onto the electrode surface by means of magnets. In order to assess the response of the electrochemical instrumentation as well as the efficiency of the magnetic collection of microbeads, the HRP enzyme was covalently immobilized directly to the surface of magnetic microbeads following the same procedure described for the immobilization of the antigens. HRP-microbeads were placed into the electrochemical cell and different concentrations of hydrogen peroxide were added using hydroquinone as a redox mediator. As the hydrogen peroxide concentration was increased, it was also observed an increase in the measured current indicating that the kinetics for the enzymatic oxidation of hydrogen peroxide could be followed amperometrically with the electrochemical instrumentation of the EMBIA platform (Fig. 3). HRP enzyme immobilized onto microbeads showed a Michaelis-Menten kinetics, as can be observed in the linearized Lineweaver-Burk plot shown in the inset of Fig. 3. These results indicate that the enzyme immobilized onto the surface of magnetic microbeads exhibits a catalytic activity, which can be amperometrically measured and explained in terms of the Michaelis-Menten kinetics.

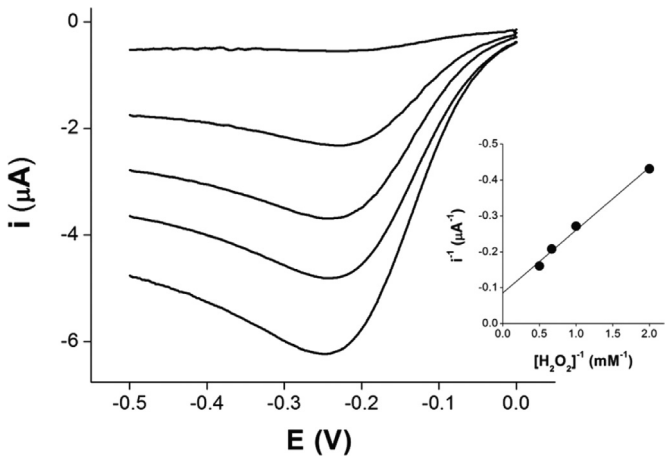

Fig. 3. Current–potential curves obtained on screen-printed electrodes using magnetic particles with immobilized HRP at a scan rate of 25 mV s^{-1}. Different concentrations of hydrogen peroxide have been used (from top to bottom: 0, 0.5, 1, 1.5 and 2 mM), while the concentration of the redox mediator hydroquinone was kept constant at 4 mM.

3.2. EMBIA platform for POC diagnosis of infectious diseases

As a proof of concept, the EMBIA platform was evaluated for the diagnosis of four infectious diseases caused by different types of microorganisms; Chagas disease caused by the parasitic protozoa *Trypanosoma cruzi*, human brucellosis caused by bacteria of the genus *Brucella* (mainly *B. melitensis*, *B. abortus* and *B. suis*), bovine brucellosis caused by *B. abortus* and foot-and-mouth disease (FMD) caused by the foot-and-mouth disease virus (FMDV). Magnetic beads coated with the corresponding recombinant antigens were incubated with a set of negative and positive control serum samples and bound antibodies were detected by the addition of anti-human or anti-bovine IgG HRP-conjugated antibodies. Peroxidase activity was electrochemically detected with the electrochemical cells-electrode cartridges and the portable potentiostat using H_2O_2 and hydroquinone as the substrate and redox mediator, respectively. The electrode potential was set at −0.23 V and the resulting current was recorded during 20 s. As shown in Fig. 4, characteristic time-current curves for positive and negative control sera were obtained. The current values for negative sera were typically around 900 nA, similar to the values obtained with PBST used as diluent of the samples, while the current values for positive sera were around 3000 and 4000 nA. These results indicate that the differences in current values at the limit current obtained at 20 s can be used to clearly differentiate positive from negative sera.

In order to demonstrate the usefulness of the EMBIA platform for diagnosis of infectious diseases, a panel of previously characterized human and bovine serum samples were analyzed (see Materials and methods). The obtained reactivity values were outlined in dotplot diagrams (Fig. 5). For the negative and positive samples the reactivity values showed no or a minimal overlap between the two sets of samples ($P < 0.0001$). In the case of human and bovine brucellosis, the results were in complete agreement with those obtained using the same antigen (OAg-AcrA) but in different platforms such as the fluorescent immunomagnetic assay and the indirect ELISA (glyco-iELISA) (Ciocchini et al., 2013; Ciocchini et al., 2014).

Taken together, these results demonstrate the potential of the EMBIA platform for PoC diagnosis of human and animal infectious diseases with an excellent signal-to-noise ratio and allowing to clearly differentiating infected from non-infected individuals or animals.

3.3. Validation of the EMBIA platform for diagnosis of Chagas disease

To validate the EMBIA platform for the diagnosis of Chagas disease, a large panel of previously characterized serum samples was tested and its diagnostic performance was compare with the fluorescent immunomagnetic and indirect ELISA assays using the same combination of antigens. The reactivity values obtained with the EMBIA, fluorescent immunomagnetic assay and iELISA are outlined in dotplot diagrams shown in Fig. 6A, B and C (upper panel). For the negative and positive samples, the reactivity values of all the assays showed a minimal overlap between the two sets of samples ($P < 0.0001$). These results indicate that using the same combination of antigens and different diagnostic platforms

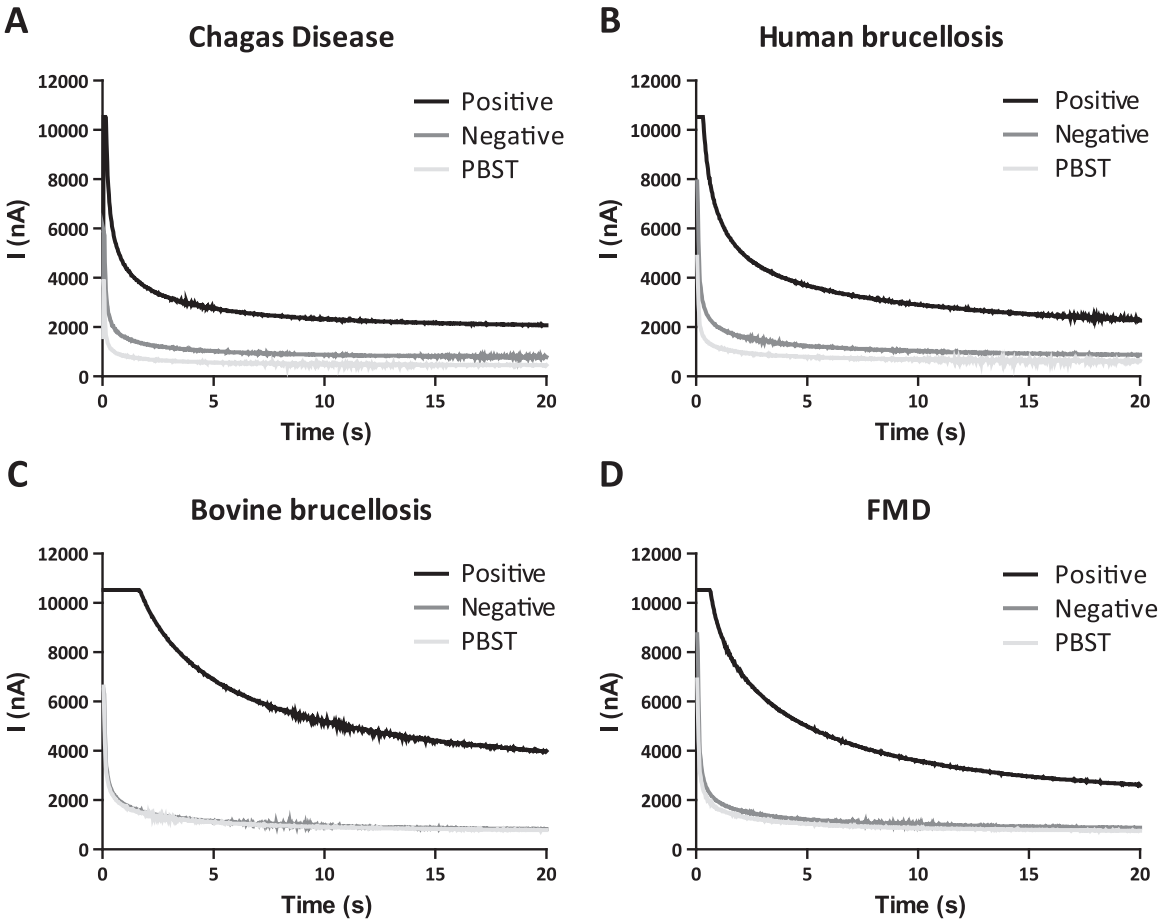

Fig. 4. EMBIA platform current transients of positive and negative sera. Representative time-current curves for positive and negative serum samples used as control sera for diagnosis of Chagas disease (A), human brucellosis (B), bovine brucellosis (C) and foot-and-mouth disease (FMD) (D). The electrode potential was set at −0.23 V and the resulting current recorded for 20 s. Current values for negative sera were typically around 900 nA similar to the values obtained with 0.01 M phosphate-buffered saline pH 7.2, 0.2% Tween 20 (PBST) used to dilute the samples (1:100 dilution).

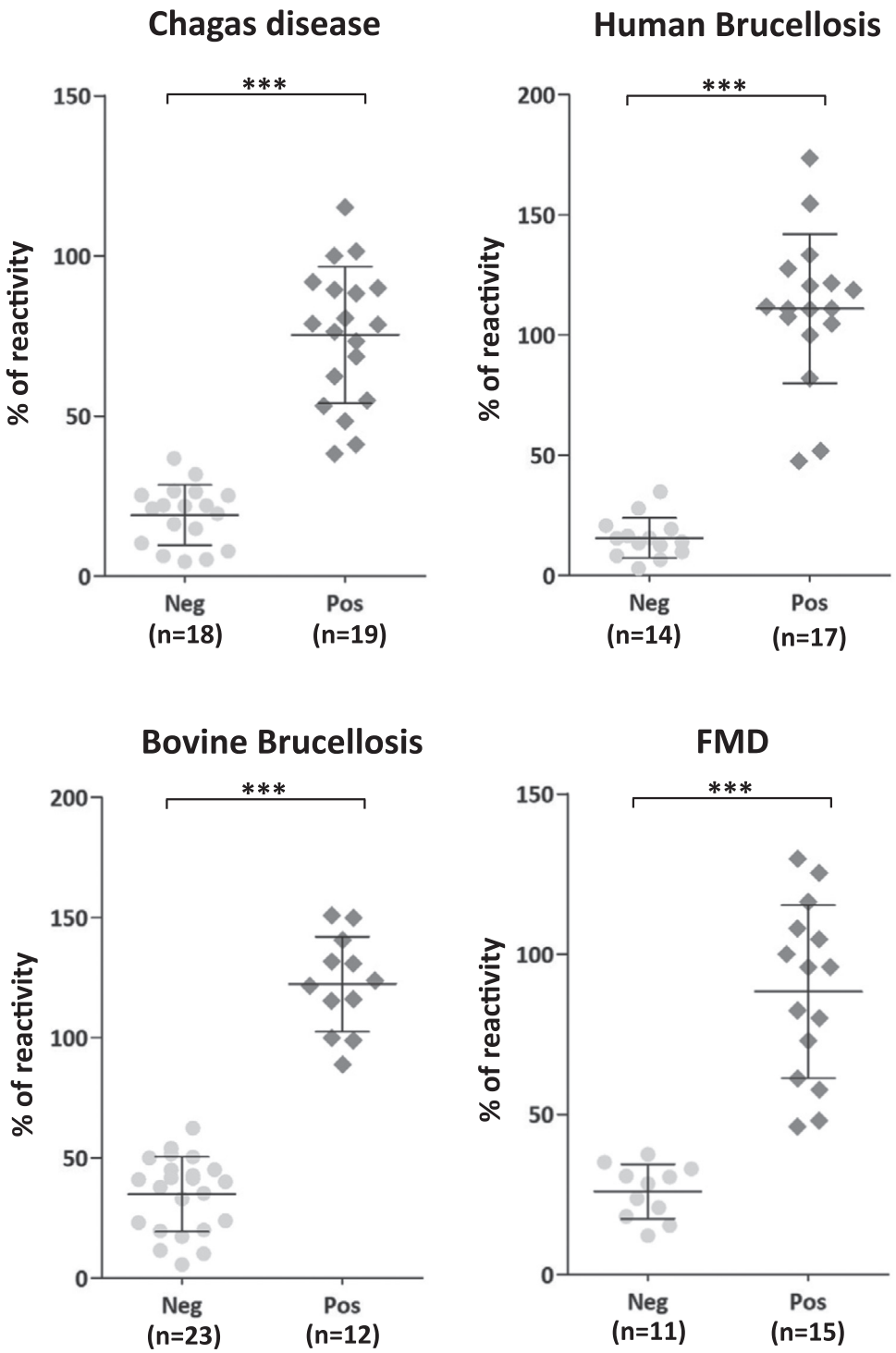

Fig. 5. Dot plot analysis of the results obtained with the EMBIA platform for diagnosis of Chagas disease, human and bovine brucellosis and foot-and-mouth disease (FMD). Magnetic beads coated with the corresponding antigens were incubated with negative and positive sera for the diagnosis of Chagas disease (A), human brucellosis (B), bovine brucellosis (C) and FMD (D). Bound antibodies were detected using HRP-conjugated goat anti-human or anti-bovine IgG antibodies. The mean and standard deviation for each group are indicated. ***, $P < 0.0001$, Mann–Whitney test.

(EMBIA, fluorescent immunomagnetic assay and iELISA) it is possible to discriminate between chronic Chagas disease patients and healthy individuals.

In order to evaluate the diagnostic performance of the EMBIA, a receiver-operating characteristic (ROC) analysis was performed. Based on the ROC results, the area under the ROC curve (AUC) values were 0.9864 (95% CI, 0.9691–1.000), 0.9991 (95% CI, 0.9975–1.000) and 0.9997 (95% CI, 0.9988–1.000) for the EMBIA, fluorescent immunomagnetic assay and iELISA, respectively (Fig. 6 A, B and C, middle panel; and Table 1). These results indicate that the EMBIA platform is highly accurate for the diagnosis of Chagas disease with a diagnostic performance similar to that of the fluorescent immunomagnetic assay and the iELISA since no significant difference between the AUC values were observed (EMBIA vs. fluorescent immunomagnetic assay, $P=0.152$; EMBIA vs. iELISA, $P=0.132$, fluorescent immunomagnetic assay vs. iELISA, $P=0.523$). Furthermore, a plot of the diagnostic sensitivity (Se) and specificity (Sp) as a function of the cut-off values (TG-ROC plot) was

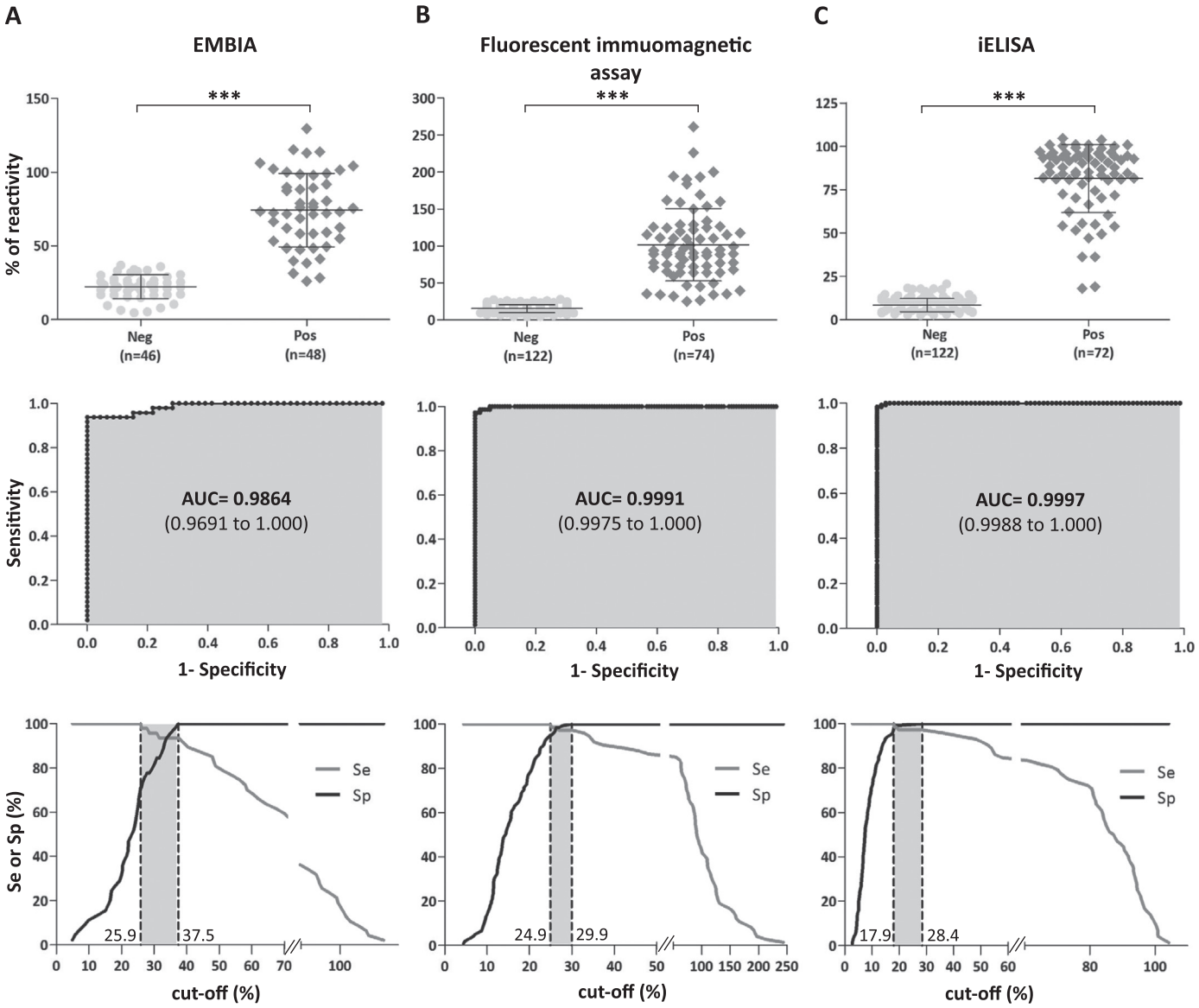

Fig. 6. Validation of the EMBIA platform for diagnosis of Chagas disease and comparison with the fluorescent immunomagnetic assay and iELISA. (A) Dot plot, ROC and TG-ROC analysis of the results obtained with the EMBIA platform. Magnetic beads coated with Ag1, Ag36, SAPA or TSSA (Chagas antigens) were mixed in equal parts and 20 μl of the mixture were incubated with the indicated human serum samples (46 negative and 48 positive sera). Bound antibodies were detected using HRP conjugated goat anti-human IgG antibodies and measuring the electric current generated after adding the substrate. (B) Dot plot, ROC and TG-ROC analysis of the results obtained with the fluorescent immunomagnetic assay. Magnetic beads coated with the Chagas antigens were incubated with the indicated serum samples (122 negative and 74 positive sera). Bound antibodies were detected using DyLight 650-conjugated goat anti-human IgG antibodies and directly reading the fluorescence. (C) Dot plot, ROC and TG-ROC analysis of the results obtained with the iELISA. ELISA plates coated with a mixture of Ag1, Ag36, SAPA and TSSA were incubated with the indicated serum samples (122 negative and 72 positive serum samples). Bound antibodies were detected using HRP-conjugated goat anti-human IgG antibodies. Results are expressed as percentage of the reactivity of the positive control serum included in each assay. The mean and standard deviation for each group are indicated. ***, $P < 0.0001$, Mann-Whitney test. AUC, area under the ROC curve; values in parentheses indicate the 95% confidence interval. The dash vertical lines in the TG-ROC curves indicate the cut-off values for which maximal Se or Sp is achieved.

performed for each assay in order to select different cut-off points so that the desired operating characteristics of the test in terms of diagnostic Se and Sp can be adjusted. This analysis allowed us to determine for each assay the cut-off value that concurrently maximizes Se and Sp, the cut-off value for which the diagnostic Se is 100% and the cut-off value that allows a 100% Sp (Fig. 6 A, B and C, lower panel; and Table 1). With the EMBIA platform, high values of diagnostic Se and Sp at the selected cut-off values were obtained. A cut-off value of 25.9% resulted in a diagnostic Se of 100% (95% CI, 92.6 to 100) and a Sp of 71.7% (95% CI, 56.5 to 84.0). At the cut-off value of 37.5%, for which the *J* index was maximal ($J=0.94$), the diagnostic Se was 93.7% (95%CI, 82.8 to 98.7) and the Sp 100% (95% CI, 92.3 to 100). These values were similar to those obtain with the fluorescent immunomagnetic and iELISA assays (Table 1). Taken together, our results demonstrate that the EMBIA platform is highly accurate for the *in situ* diagnosis of Chagas disease displaying a diagnostic performance similar to that obtained with the fluorescent immunomagnetic assay and the classical ELISA platform using the same combination of recombinant antigens.

Different technologies were combined and integrated in the EMBIA platform including microelectronics, electrochemistry, the use of magnetic beads and biotechnology, among others. Microelectronics and electrochemical transducers allow the development of small size, low cost and robust biosensors with a high

Table 1
AUC values, sensitivity, specificity and Youden's index of the tests calculated for different cut-off values[a].

Assay[b]	AUC[c]	Cut-off (%)	Se (%)[d]	Sp (%)[d]	*J*[e]
EMBIA	0.9864 (0.9691–1.000)	> 25.9	**100**[f] (92.6–100)	71.7 (56.5–84.0)	0.72
		> 37.5	93.7 (82.8–98.7)	**100** (92.3–100)	**0.94**
Fluorescent immunomagnetic assay	0.9991 (0.9975–1.000)	> 24.9	**100** (95.1–100)	95.1 (89.6–98.2)	0.95
		> 29.9	97.3 (90.6–99.7)	**100** (97.0–100)	**0.97**
iELISA	0.9997 (0.9989–1.000)	> 17.9	**100** (95.0–100)	98.3 (94.1–99.8)	**0.98**
		> 28.4	97.2 (90.3–99.7)	**100** (96.9–100)	0.97

[a] The analysis was performed using serum samples obtained from patients with Chagas disease and healthy blood donors (see Materials and methods).
[b] EMBIA, electrochemical enzyme-linked magnetic beads immunoassay.
[c] AUC, area under the ROC curve. Values in parentheses indicate the 95% confidence interval.
[d] Se (%), sensitivity (TP/TP+FN) × 100; Sp (%), specificity (TN/TN+FP) × 100. Values in parentheses indicate the 95% confidence interval.
[e] *J*, Youden's index (Se+Sp−1).
[f] Maximum values for Se, Sp and *J* are indicated in bold.

degree of integration. Additionally, magnetic microbeads were used in this platform as a solid-phase support for the antigens, which simplifies the assay since the incubations and removal of unwanted sample constituents can be performed by a simple magnetic separation step without the need of centrifugation and with a minimal loss of the target material. Furthermore, the use of microbeads allowed the reduction of the time of the assay and the volume of sample required for the analysis and even more importantly, to combine different antigens in a controlled and standardized manner as in the case for the diagnosis of Chagas disease. Finally, biotechnology, in particular genetic engineering and bacterial glycoengineering, has allowed us to produce and purify large amounts of highly specific recombinant antigens at relatively low cost. By combining these technologies, we were able to develop a portable, robust and low cost device for PoC diagnosis of multiple human and animal infectious diseases caused by different etiological agents such as parasitic protozoa, bacteria and viruses. Furthermore, we have performed a complete validation of the EMBIA platform for the diagnosis of Chagas disease displaying an excellent diagnostic performance. Further work will be required to validate the EMBIA platform in the field and for the diagnosis of other infectious or non-infectious diseases as well as for the detection and/or quantification of biomarkers.

4. Conclusions

We have developed and evaluated an electrochemical magnetic beads-based biosensor (EMBIA platform) for PoC serodiagnosis of human (Chagas disease and human brucellosis) and animal (bovine brucellosis and FMD) infectious diseases caused by different types of microorganisms. The diagnostic performance of the EMBIA platform was compared to the well-established iELISA and a fluorescent immunomagnetic assay, displaying excellent results. Due to its portability, short incubation times, the possibility to perform 8 readings in less than 3 min (20 s per reading), simplicity and high accuracy, we propose that the EMBIA platform technology can be applied to PoC diagnosis of these and other infectious diseases at resource-constrained and primary care settings.

Acknowledgements

This work was supported by PICT Start Up 2010/0144 (Préstamo BID 2437) and FONARSEC NANO 2010 No. 005 Grants from Agencia Nacional de Promoción Científica y Tecnológica (ANPCyT), Argentina.

Appendix A. Supplementary material

Supplementary data associated with this article can be found in the online version at doi:10.1016/j.bios.2016.01.021.

References

Balouz, V., Camara Mde, L., Canepa, G.E., Carmona, S.J., Volcovich, R., Gonzalez, N., Altcheh, J., Aguero, F., Buscaglia, C.A., 2015. Mapping antigenic motifs in the trypomastigote small surface antigen from Trypanosoma cruzi. Clin. Vaccine Immunol. 22 (3), 304–312.
F.-G. Bănică, 2012. Chemical Sensors and Biosensors: Fundamentals and Applications.
Buscaglia, C.A., Alfonso, J., Campetella, O., Frasch, A.C., 1999. Tandem amino acid repeats from Trypanosoma cruzi shed antigens increase the half-life of proteins in blood. Blood 93 (6), 2025–2032.
Ciocchini, A.E., Rey Serantes, D.A., Melli, L.J., Iwashkiw, J.A., Deodato, B., Wallach, J., Feldman, M.F., Ugalde, J.E., Comerci, D.J., 2013. Development and validation of a novel diagnostic test for human brucellosis using a glyco-engineered antigen coupled to magnetic beads. PLoS Negl. Trop. Dis. 7 (2), e2048.
Ciocchini, A.E., Serantes, D.A., Melli, L.J., Guidolin, L.S., Iwashkiw, J.A., Elena, S., Franco, C., Nicola, A.M., Feldman, M.F., Comerci, D.J., Ugalde, J.E., 2014. A bacterial engineered glycoprotein as a novel antigen for diagnosis of bovine brucellosis. Vet. Microbiol. 172 (3–4), 455–465.
De Marchi, C.R., Di Noia, J.M., Frasch, A.C., Amato Neto, V., Almeida, I.C., Buscaglia, C. A., 2011. Evaluation of a recombinant Trypanosoma cruzi mucin-like antigen for serodiagnosis of Chagas' disease. Clin. Vaccine Immunol. 18 (11), 1850–1855.
Di Noia, J.M., Buscaglia, C.A., De Marchi, C.R., Almeida, I.C., Frasch, A.C., 2002. A Trypanosoma cruzi small surface molecule provides the first immunological evidence that Chagas' disease is due to a single parasite lineage. J. Exp. Med. 195 (4), 401–413.
Dorothee Grieshaber, R.M., Voros, Janos, Reimhult, Erik, 2008. Electrochemical biosensors – sensor principles and architectures. Sensors 8, 1400–1458.
Girosi, F., Olmsted, S.S., Keeler, E., Hay Burgess, D.C., Lim, Y.W., Aledort, J.E., Rafael, M.E., Ricci, K.A., Boer, R., Hilborne, L., Derose, K.P., Shea, M.V., Beighley, C.M., Dahl, C.A., Wasserman, J., 2006. Developing and interpreting models to improve diagnostics in developing countries. Nature 444 (Suppl. 1), S3–S8.
Greiner, M., Gardner, I.A., 2000. Application of diagnostic tests in veterinary epidemiologic studies. Prev. Vet. Med. 45 (1–2), 43–59.
Greiner, M., Sohr, D., Gobel, P., 1995. A modified ROC analysis for the selection of cut-off values and the definition of intermediate results of serodiagnostic tests. J. Immunol. Methods 185 (1), 123–132.
Hay Burgess, D.C., Wasserman, J., Dahl, C.A., 2006. Global health diagnostics. Nature 444 (Suppl. 1), 1–2.
Holford, T.R., Davis, F., Higson, S.P., 2012. Recent trends in antibody based sensors. Biosens. Bioelectron. 34 (1), 12–24.
Iwashkiw, J.A., Fentabil, M.A., Faridmoayer, A., Mills, D.C., Peppler, M., Czibener, C., Ciocchini, A.E., Comerci, D.J., Ugalde, J.E., Feldman, M.F., 2012. Exploiting the Campylobacter jejuni protein glycosylation system for glycoengineering vaccines and diagnostic tools directed against brucellosis. Microb. Cell. Fact. 11, 13.
Kuramitz, H., 2009. Magnetic microbead-based electrochemical immunoassays. Anal. bioanal. Chem. 394 (1), 61–69.
Peeling, R.W., Mabey, D., 2010. Point-of-care tests for diagnosing infections in the developing world. Clin. Microbiol. Infect. 16 (8), 1062–1069.
Song, Y., Huang, Y.Y., Liu, X., Zhang, X., Ferrari, M., Qin, L., 2014. Point-of-care technologies for molecular diagnostics using a drop of blood. Trends Biotechnol. 32 (3), 132–139.
Swets, J.A., 1988. Measuring the accuracy of diagnostic systems. Science 240 (4857), 1285–1293.
Urdea, M., Penny, L.A., Olmsted, S.S., Giovanni, M.Y., Kaspar, P., Shepherd, A., Wilson, P., Dahl, C.A., Buchsbaum, S., Moeller, G., Hay Burgess, D.C., 2006. Requirements for high impact diagnostics in the developing world. Nature 444 (Suppl. 1), S73–S79.

Supplementary information

Material and methods

Trypanosoma cruzi antigens. SAPA (shed-acute phase antigen) (Affranchino et al. 1989) is a repetitive domain present in the C-terminus of trans-sialidase, a multitasking *T. cruzi* virulence factor expressed on the surface of infective cell-derived trypomastigote forms (Dc-Rubin and Schenkman 2012). The particular amino acid sequence of SAPA defines an intricate B-cell epitope structure (Alvarez et al. 2001; Pitcovsky et al. 2002) and, at the same time, stabilizes trans-sialidase activity in the bloodstream upon its secretion (Alvarez et al. 2004; Buscaglia et al. 1999). SAPA triggers a robust antibody response during acute infections in humans, and has been validated for the early recognition of congenital cases (Reyes et al. 1990; Russomando et al. 2010). Antigen 36 (Ag36) is a repetitive antigen expressed in multiple parasite developmental stages and recognized by T. cruzi-infected individuals coursing both the acute and the chronic phase of the disease (Ibanez et al. 1988). Ag36 (also known as JL9 or MAP (Frasch et al. 1988)) is a cytoplasmic molecule of unknown function displaying marginal homology to microtubule-associated proteins. Antigen 1 (Ag1, also known as FRA, JL7 or H49 (Frasch et al. 1988)) is also a repetitive molecule of unknown function, that localizes underneath the flagellar pocket membrane throughout the parasite life-cycle (Cotrim et al. 1995). At variance with antigens described above, antibody recognition of Ag1 is restricted to chronic infections (Ibanez et al. 1988). TSSA (trypomastigote small surface antigen) is a small and polymorphic mucin-type protein present on the surface of cell-derived trypomastigote forms that contributes to their interaction with mammalian cells (Canepa et al. 2012). TSSA has been recently validated as a promising reagent for immunodiagnosis of chronic Chagas disease (Balouz et al. 2015; De Marchi et al. 2011; Di Noia et al. 2002).

Table S1. Plasmids and strains used in this work.

Plasmids/Strains	Description/Characteristic[a]	Source
Plasmids		
pGEX1λT	Expression vector, Amp^R	GE Healthcare Life Sciences
pGEX2T	Expression vector, Amp^R	GE Healthcare Life Sciences
pET22b(+)	Expression vector, Amp^R	Novagen
pTrcHis-TS-Ag1	Encodes quimeric*trans-sialidase*-Ag1 hexa-His-tagged under control of T7 promoter, in pTrcHisA vector, Amp^R	(Buscaglia et al. 1999)
pTrcHis-TS-Ag36	Encodes quimeric*trans-sialidase*-Ag36 hexa-His-tagged under control of T7 promoter, in pTrcHisA vector, Amp^R	(Buscaglia et al. 1999)
pTrcHis-TS-SAPA	Encodes quimeric*trans-sialidase*-SAPA hexa-His-tagged under control of T7 promoter, in pTrcHisA vector, Amp^R	(Buscaglia et al. 1999)
pGEX2T-TSSA	Encodes TSSA VI gene fused to GST under control of T7 promoter, in pGEX2T, Amp^R	(De Marchi et al. 2011)
pGEX1λT-Ag1	Encodes antigen 1 gene fused to GST under control of T7 promoter, in pGEX1λT, Amp^R	This work
pGEX1λT-Ag36	Encodes antigen 36 gene fused to GST under control of T7 promoter, in pGEX1λT, Amp^R	This work
pGEX1λT-SAPA	Encodes antigen SAPA gene fused to GST under control of T7 promoter, in pGEX1λT, Amp^R	This work
pMH5	Encodes AcrA gene fused to His tag under control of constitutive promoter in pACYC184, Cm^R	(Feldman et al. 2005)
pMAF10	Encodes PglB gene fused to HA tag under control of arabinose promoter in pBAD, Tmp^R	(Feldman et al. 2005)
pET22-3ABC	Encodes 3ABC gene fused to 6x histidine tag under control of T7 promoter in pET22b(+), Amp^R	This work
Strains		
Escherichia coli DH5αF'IQ™	F-ϕ80lacZΔM15 Δ(lacZYA-argF) U169 recA1 endA1 hsdR17 (rk-, mk+) phoAsupE44 λ- thi-1 gyrA96 relA1/F´ proAB+ lacIqZΔM15 zzf::Tn5 [Km^R].	Life Technologies
Escherichia coli BL21-CodonPlus (DE3)-RP	*E. coli* B F- ompThsdS(rB-mB-) dcm+ Tetr gal l(DE3) endAHte [argUproLCm^R]	Agilent Technologies
YeO9	*Yersinia enterocolitica* O:9, wild type strain	(Iwashkiw et al. 2012)

[a]Cm, chloramphenicol; Amp, ampicillin; Tmp, trimethoprim; Km, kanamycin.

References

Affranchino, J.L., Ibanez, C.F., Luquetti, A.O., Rassi, A., Reyes, M.B., Macina, R.A., Aslund, L., Pettersson, U., Frasch, A.C., 1989. Identification of a Trypanosoma cruzi antigen that is shed during the acute phase of Chagas' disease. Mol Biochem Parasitol 34(3), 221-228.

Alvarez, P., Buscaglia, C.A., Campetella, O., 2004. Improving protein pharmacokinetics by genetic fusion to simple amino acid sequences. The Journal of biological chemistry 279(5), 3375-3381.

Alvarez, P., Leguizamon, M.S., Buscaglia, C.A., Pitcovsky, T.A., Campetella, O., 2001. Multiple overlapping epitopes in the repetitive unit of the shed acute-phase antigen from Trypanosoma cruzi enhance its immunogenic properties. Infection and immunity 69(12), 7946-7949.

Balouz, V., Camara Mde, L., Canepa, G.E., Carmona, S.J., Volcovich, R., Gonzalez, N., Altcheh, J., Aguero, F., Buscaglia, C.A., 2015. Mapping antigenic motifs in the trypomastigote small surface antigen from Trypanosoma cruzi. Clinical and vaccine immunology : CVI 22(3), 304-312.

Buscaglia, C.A., Alfonso, J., Campetella, O., Frasch, A.C., 1999. Tandem amino acid repeats from Trypanosoma cruzi shed antigens increase the half-life of proteins in blood. Blood 93(6), 2025-2032.

Canepa, G.E., Degese, M.S., Budu, A., Garcia, C.R., Buscaglia, C.A., 2012. Involvement of TSSA (trypomastigote small surface antigen) in Trypanosoma cruzi invasion of mammalian cells. Biochem J 444(2), 211-218.

Cotrim, P.C., Paranhos-Baccala, G., Santos, M.R., Mortensen, C., Cano, M.I., Jolivet, M., Camargo, M.E., Mortara, R.A., Da Silveira, J.F., 1995. Organization and expression of the gene encoding an immunodominant repetitive antigen associated to the cytoskeleton of Trypanosoma cruzi. Mol Biochem Parasitol 71(1), 89-98.

Dc-Rubin, S.S., Schenkman, S., 2012. T rypanosoma cruzi trans-sialidase as a multifunctional enzyme in Chagas' disease. Cellular microbiology 14(10), 1522-1530.

De Marchi, C.R., Di Noia, J.M., Frasch, A.C., Amato Neto, V., Almeida, I.C., Buscaglia, C.A., 2011. Evaluation of a recombinant Trypanosoma cruzi mucin-like antigen for serodiagnosis of Chagas' disease. Clinical and vaccine immunology : CVI 18(11), 1850-1855.

Di Noia, J.M., Buscaglia, C.A., De Marchi, C.R., Almeida, I.C., Frasch, A.C., 2002. A Trypanosoma cruzi small surface molecule provides the first immunological evidence that Chagas' disease is due to a single parasite lineage. J Exp Med 195(4), 401-413.

Feldman, M.F., Wacker, M., Hernandez, M., Hitchen, P.G., Marolda, C.L., Kowarik, M., Morris, H.R., Dell, A., Valvano, M.A., Aebi, M., 2005. Engineering N-linked protein glycosylation with diverse O antigen lipopolysaccharide structures in Escherichia coli. Proc Natl Acad Sci U S A 102(8), 3016-3021.

Frasch, A.C., Affranchino, J.L., Ibanez, C.F., Reyes, M.B., Macina, R.A., Luquetti, A.O., Rassi, A., Aslund, L., Pettersson, U., 1988. Analysis of cloned Trypanosoma cruzi proteins that are antigenic during the acute and chronic phase of Chagas' disease. Mem Inst Oswaldo Cruz 83 Suppl 1, 345-346.

Ibanez, C.F., Affranchino, J.L., Macina, R.A., Reyes, M.B., Leguizamon, S., Camargo, M.E., Aslund, L., Pettersson, U., Frasch, A.C., 1988. Multiple Trypanosoma cruzi antigens containing tandemly repeated amino acid sequence motifs. Mol Biochem Parasitol 30(1), 27-33.

Iwashkiw, J.A., Fentabil, M.A., Faridmoayer, A., Mills, D.C., Peppler, M., Czibener, C., Ciocchini, A.E., Comerci, D.J., Ugalde, J.E., Feldman, M.F., 2012. Exploiting the Campylobacter jejuni protein glycosylation system for glycoengineering vaccines and diagnostic tools directed against brucellosis. Microb Cell Fact 11, 13.

Pitcovsky, T.A., Buscaglia, C.A., Mucci, J., Campetella, O., 2002. A functional network of intramolecular cross-reacting epitopes delays the elicitation of neutralizing antibodies to Trypanosoma cruzi trans-sialidase. J Infect Dis 186(3), 397-404.

Reyes, M.B., Lorca, M., Munoz, P., Frasch, A.C., 1990. Fetal IgG specificities against Trypanosoma cruzi antigens in infected newborns. Proc Natl Acad Sci U S A 87(7), 2846-2850.

Russomando, G., Sanchez, Z., Meza, G., de Guillen, Y., 2010. Shed acute-phase antigen protein in an ELISA system for unequivocal diagnosis of congenital Chagas disease. Expert Rev Mol Diagn 10(6), 705-707.

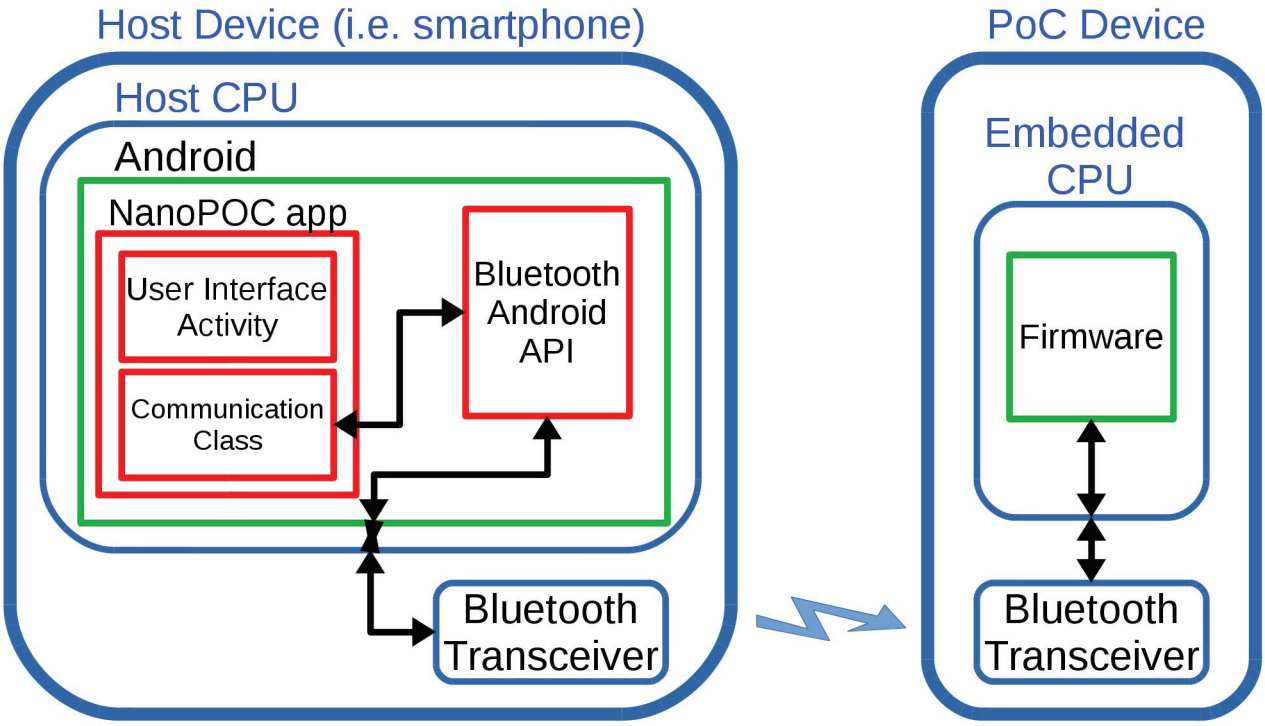
Host Device (i.e. smartphone)
Host CPU
Android
NanoPOC app
User Interface Activity
Communication Class
Bluetooth Android API
Bluetooth Transceiver
PoC Device
Embedded CPU
Firmware
Bluetooth Transceiver

Figure S1